Mixed Tb/Dy coordination ladders based on tetra(carboxymethyl)thiacalix[4]arene: a new avenue towards luminescent molecular nanomagnets

Alexander Ovsyannikov, Ivan Khariushin, S. Solovieva, I. Antipin, H. Komiya, Nicolas Marets, H. Tanaka, H. Ohmagari, M. Hasegawa, J. Zakrzewski, et al.

ARTICLE

Mixed Tb/Dy coordination ladders based on tetra(carboxymethyl)thiacalix[4]arene: a new avenue towards luminescent molecular nanomagnets

Received 00th January 20xx,
Accepted 00th January 20xx

DOI: 10.1039/x0xx00000x

A.S. Ovsyannikov,*[a] I.V. Khariushin,[b] S.E. Solovieva,[a] I.S. Antipin,[b] H. Komiya,[c] N. Marets,[c] H. Tanaka,[c] H. Ohmagari,[c] M. Hasegawa,[c] J. J. Zakrzewski,[d] S. Chorazy,[d] N. Kyritsakas,[e] M. W. Hosseini,[e] S. Ferlay*[e]

Macrocyclic ligands calix[4]arene (L**1**) and their sulphur-containing analogue, thia[4]calixarene (L**2**), are promising precursors for functional molecular materials as they offer rational functionalization by various organic groups. Here, were present the first example of lanthanide based Coordination Polymers, build from the macrocyclic thiacalix[4]arene backbone bearing four carboxylic moieties, ligand **H_4L3**. The combination of **H_4L3** with Tb^{3+} and Dy^{3+} cations leads to the formation of 1D ladder-type coordination polymers, of formula $[Ln^{III}$**HL3**$DMF_3]\bullet$(DMF), where DMF=dimethylformamide and Ln = Tb or Dy, **HL3-Tb** and **HL3-Dy**, resulting from the coordination of the lanthanide cations by the partially deprotonated ligand **$HL3^{3-}$** behaving as a T-shape connector. The coordination sphere of the metal is completed by coordinated DMF solvent molecules. By combining both Tb^{3+} and Dy^{3+} cations, isostructural heterobimetallic solid solutions **HL3-$Tb_{1-x}Dy_x$** have also been prepared. **HL3-Tb** and **HL3-Dy** show visible light photoluminescence originating from f-f electronic transitions of pale green emissive Tb^{3+} and pale yellow emissive Dy^{3+} with the efficient sensitization by functionalized thia[4]calixarene ligand **HL3**. In the **HL3-$Tb_{1-x}Dy_x$** solid solutions, the Tb/Dy ratio governs both the emission colour as well as thee emission quantum yield, reaching even 28% at room temperature for **HL3-Tb**. Moreover, **HL3-Dy** exhibits a slow magnetic relaxation effect related to the magnetic anisotropy of dodecahedral Dy^{3+} complexes, well isolated in the crystal lattice by expanded organic spacers.

Introduction

Coordination polymers (CPs),[1,2] MOFs[3] or molecular networks[4,5] are molecular architectures offering properties such as gas storage,[6,7] catalysis,[8,9] magnetism[10,11] or luminescence[12,13,14] for example. The generation of such molecular species is based on the formation of coordination bonds between organic coordinating ligands and metal centres or complexes.[15] A large number of coordination polymers displaying different connectivity patterns has been generated using different types of polytopic ligands and metals.

Concerning luminescence properties[12] of CPs, special attention has been devoted to lanthanide based CPs,[16,17,18] owing to their outstanding photoluminescence originating from triplet excited states of f–f transitions. Lanthanide based CPs may find applications in luminescent sensing, light-emitting together with photonics,[19,20,21] using ligands presenting strong antenna effect,[22] allowing the energy transfer from the organic ligand to the metal. The use of macrocyclic ligands for the formation of such assemblies has been documented,[23] however, most of the reported examples are mainly related to porphyrine based lanthanide CPs.[24]

Concerning magnetic properties of Lanthanide based CPs, examples of molecular nanomagnets have been provided.[25,26,27] In addition, LnCPs may combine both SMM behaviour and tuneable photoluminescence, as shown recently.[28,29,30]

For building new CPs based on macrocycles, the use of calixarene derivatives represents a nice alternative. Calix[4]arenes[31,32,33] are macrocyclic compounds composed of four phenolic moieties bridged by methylene groups: “classical” calix[4]arene, CA, **L1** (Figure 1), sulphur atoms, in the case of thiacalix[4]arene TCA, **L2** (Figure 1),[34] bearing hydroxyl or mercapto groups (tetramercaptothiacalix[4]arene (TMTCA).[35,36] These molecules can be easily modified by functionalization of the upper and/or lower rims of the macrocyclic scaffold. They may adopt four different conformations (*cone*, *partial cone*, *1,2-alternate* and *1,3-alternate*) that make these compounds attractive precursors for the design of molecular networks. The generation of coordination polymers with various dimensionalities using tetrasubstituted

[a] *Arbuzov Institute of Organic and Physical Chemistry, FRC Kazan Scientific Center, Russian Academy of Sciences, Arbuzov str. 8, Kazan 420088, RUSSIAN FEDERATION; osaalex2007@rambler.ru*
[b] *Kazan Federal University, Kremlevskaya str. 18, Kazan 420008, RUSSIAN FEDERATION.*
[c] *College of Science and Engineering, Aoyama Gakuin University, 5-10-1 Fuchinobe, Chuo-ku, Sagamihara, Kanagawa 252-5258, JAPAN.*
[d] *Faculty of Chemistry, Jagiellonian University, Gronostajowa 2, 30-387 Krakow, POLAND.*
[e] *Université de Strasbourg, CNRS, CMC UMR 7140, F-67000 Strasbourg, FRANCE; ferlay@unistra.fr*

† Footnotes relating to the title and/or authors should appear here.
Electronic Supplementary Information (ESI) available: Analysis using Shape program, measured cells for the solid solutions, EDS analysis for the solid solutions, excitation spectra, Absolute luminescence quantum yields, decay profile analysis and details of magnetic measurements. See DOI: 10.1039/x0xx00000x

(tetramercapto)(thia)calix[4]arene derivatives bearing different coordinating sites is well documented.[37]

Functionalized calix[6]arene bearing amide groups, or calix[8]arene,[38,39] or unsubstituted calix[4]arene and thiacalix[4]arene derivatives in cone conformation,[40,41,42,43] combined with lanthanides salts or mixtures of 3d/4f, [44,45,46,47,48,49,50,51] different types of clusters have been obtained. Among them, the use of calixarenes bearing carboxylic coordinating sites, for which the lanthanides cations present a great affinity, has been reported for the formation of isolated complexes.[52,53]

It is important to note that, up to date, only few lanthanide based coordination networks involving calixarene derivatives were reported: they were mainly formed by tetrasulfonate derivatives of (thia)calix[4]arenes in *cone* conformation.[54,55,56,57] To the best of our knowledge, no examples involving carboxylate derivatives or (thia)calix[4]arenes in *1,3-alternate* conformation have been reported so far.

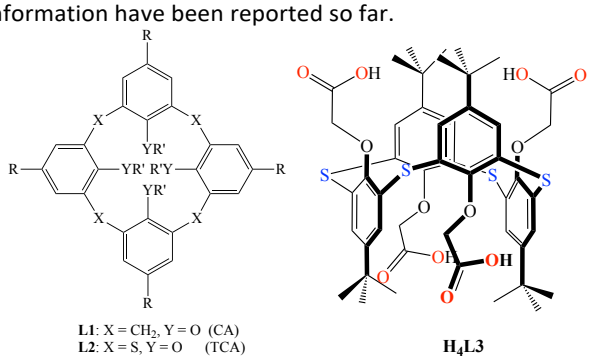

Figure 1. Calix[4]arene (**L1,** CA) and thiacalix[4]arene (**L2,** CA) and tetramethylenecarboxylate derivative of thiacalix[4]arene (**H_4L3**) adopting a *1,3*-alternate conformation.

Several calixarene derivatives bearing carboxylic/ate coordinating groups have been described. Among them, compound **H_4L3** and its use for the formation of coordination polymers with 3d metals such as Co(II) or Mn(II) and ancillary ligands.[58,59] The analogous ligand without *tert*-butyl groups has been used for the formation of coordination polymers with Ag^+, Ni^{2+}, Co^{2+}, and Zn^{2+} together with K^+.[60,61] TMTCA derivatives, based coordination polymers using 3d metals have also been reported,[62] together with hydrogen bonded networks.[63]

In this contribution, we report on the structure of a series of isostructural new 1D lanthanide based coordination networks derived from tetrasubstituted TCA in *1,3*-alternate conformation and bearing carboxylate moieties (**$HL3^{3-}$**). A series of isostructural, homo and heterometallic lanthanide based periodic architecture (Dy/Tb, because of the isostructurality of the related CPs), has been prepared. Mixing lanthanide cations in solid solutions coordination networks can lead to the combination of two phosphorescent centres with large emission differences, which is a common strategy to gain self-referenced luminescence. Heteronuclear lanthanide Gd/Eu or La/Tb, Tb/Eu or Dy/Ln polymers are usually reported for the fine tuning (colour and brightness) of the corresponding luminescence properties.[64,65,66] Generally mixed Eu/Tb compounds, due to the optimal energy match between both lanthanide cations, allows energy transfer in mixed coordination polymers.[67,68,69,70,71,72] But tuneable emission can also arise using mixed Tb/Dy coordination compounds.[73]

The ligand fluorescence and Dy^{3+} and Tb^{3+} phosphorescence were thoroughly studied in the solid state in the corresponding (Dy/Tb) solid solutions. In addition, the magnetic properties of the anisotropic Dy^{3+} compound were investigated in details.

Results and discussion

Synthesis and structural details

The synthesis of compound **H_4L3** has been achieved following the previously reported procedure consisting in a nucleophilic substitution reaction between TCA with ethyl bromoacetate in presence of Cs_2CO_3 in acetone, followed by hydrolysis under basic conditions using LiOH in a THF/H_2O mixture.[63,74,75] The combination of compound **H_4L3** with lanthanide (III) nitrate salts (Ln = Tb or Dy) under solvothermal conditions in DMF (see experimental part), led to formation of isostructural 1D coordination networks. Structural investigations were carried out using X-ray diffraction on both single crystals of **HL3-Ln** (Ln = Dy and Tb). The formula derived from the analysis was found to be $[C_{48}H_{53}O_{12}S_4Ln(C_3H_7NO)_3]\bullet(C_3H_7NO)$ ($[Ln^{III}\mathbf{HL3}DMF_3]\bullet(DMF)$, Ln = Dy or Tb), as shown in the crystallographic table 1. The ligand/metal ratio is 1/1.

Crystals are composed of **$HL3^{3-}$** in its tris-deprotonated form (see table 2 for C-O distances), the trivalent Ln cation (Ln(III)) and four DMF solvent molecules. The description of the structure in the solid state is reported here below only for **HL3-Tb**. The Terbium atom is octacoordinated and surrounded by oxygen atoms. Two carboxylate moieties coordinate the lanthanide in a bidentate mode and the third carboxylate presents a monodentate coordination mode. 3 oxygen atoms belonging to three DMF molecules complete the coordination sphere of Tb (Figure 2c). Using the SHAPE program[76], the geometry around the Tb centres has been shown to be deformed triangular dodecahedron, as shown in ESI.

The crystal contains also a non-coordinated DMF molecule occupying the interstices between antiparallel 1D coordination networks without any specific interactions with them. The terbium atoms are acting as a T -shape connector, connecting three carboxylate groups belonging to three adjacent ligands **$HL3^{3-}$**, leading to a double chain ladder-like structure (Figures 2a, b and schematically represented in d). Consequently, the fourth carboxylic group remains protonated without interactions with the other components of the crystal.

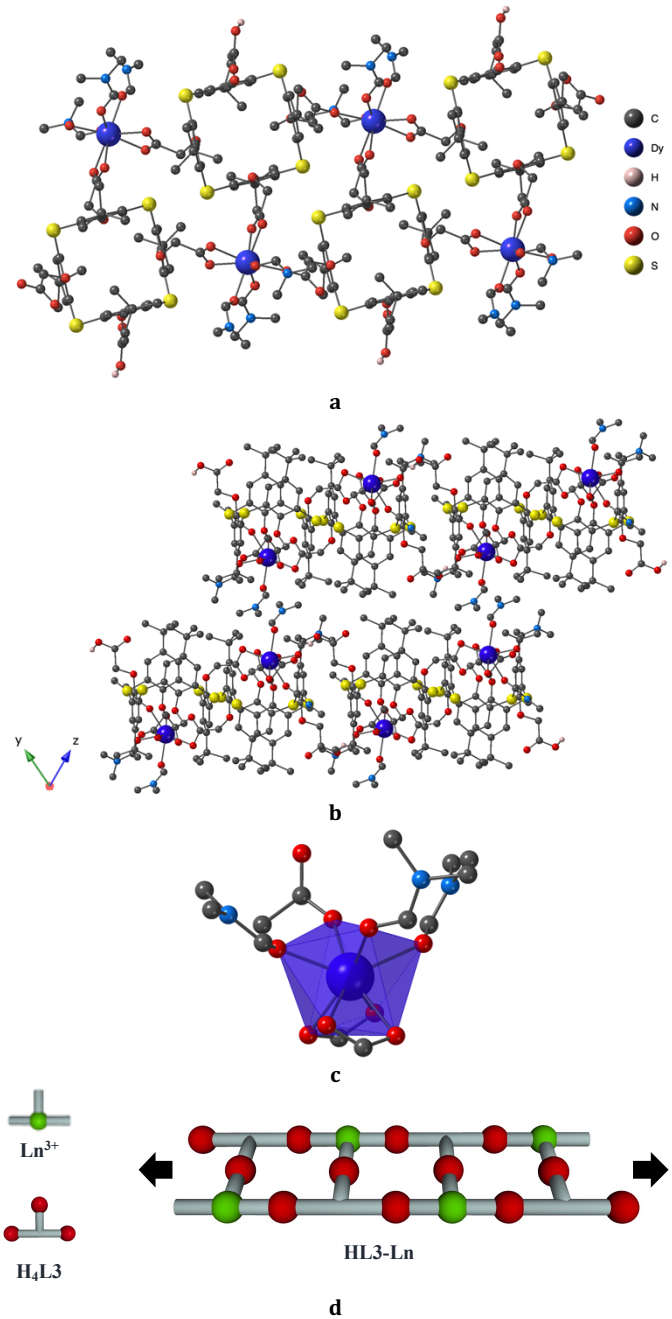

Figure 2. (a) A portion of crystal structure of **HL3-Tb**, (b) crystal packing of **HL3-Tb**, (c) coordination environment of Ln^{3+} and (d) schematic representation of connectivity for **HL3-Tb**.

As expected, different C-O distances for carboxylic moieties of $\mathbf{HL3}^{3-}$ are observed, revealing the presence of one non-coordinating carboxylic group and three coordinating carboxylate moieties (see table 2).

Within the 1-D arrays, the shortest Tb-Tb distances is equal to 11.879(3) Å and the packing of the 1D networks in the *yOz* plane (Figure 2b, packing along the *a* axis) leads to a shorter Tb-Tb distance of 7.836(4) Å between two Tb atoms belonging to two different chains.

Table 2. Selected bond distances (Å) for **HL3**-Dy and **HL3**-Tb

	HL3-Dy	HL3-Tb
C-O (carboxyl-ate/-ic)	1.232(5) and 1.273(5)	1.215(4) and 1.269(4)
	1.239(5) and 1.268(4)	1.253(4) and 1.258(4)
	1.254(5) and 1.261(5)	1.243(4) and 1.259(4)
	1.189(5) and 1.323(5) (carboxylic)	1.194(5) and 1.320(5) (carboxylic)
Ln-O (DMF)	2.354(3)	2.355(3)
	2.366(3)	2.369(2)
	2.380(3)	2.395(3)
Ln-O (Carboxylate)	2.256(3)	2.277(2)
	2.380(3)	2.393(3)
	2.393(3)	2.411(3)
	2.404(3)	2.418(3)
	2.438(3)	2.440(2)

Since both compounds **HL3-Dy** and **HL3-Tb** are isostructural (which was not the case for Gd and Eu analogues, for example), solid solutions of formula $\mathbf{HL3\text{-}Tb_{1-x}Dy_x}$ have been prepared, using the same synthetic procedure as the one used for **HL3-Dy** and **HL3-Tb** (see experimental section). While in our case, the related Eu compound obtained with $\mathbf{H_4L3}$ was found to be not isostructural with **HL3**-Tb or **HL3**-Dy.

Starting from different experimental Dy/Tb ratios, microcrystalline compounds of the following formula: $\mathbf{HL3\text{-}Tb_{0.07}Dy_{0.93}}$, $\mathbf{HL3\text{-}Tb_{0.20}Dy_{0.80}}$, $\mathbf{HL3\text{-}Tb_{0.42}Dy_{0.58}}$, $\mathbf{HL3\text{-}Tb_{0.67}Dy_{0.33}}$ and $\mathbf{HL3\text{-}Tb_{0.95}Dy_{0.05}}$ have been obtained.

The structure of the solid solution was investigated by XRPD as shown in Figure 3 (for cell parameters determinations of the corresponding single crystals see table S1, Supplementary Information). XRPD clearly demonstrated the structural homogeneity of the phase of the formed coordination compounds. All $\mathbf{HL3\text{-}Tb_{1-x}Dy_x}$ solid solutions are isostructural and display the same structure as observed for **HL3-Tb** or **HL3-Dy**. Since there is only one type of crystallographically independent Ln ion in the unit cell, owing to close size of the two lanthanide cations, one may assume a statistical distribution of the lanthanide cations in the crystal.

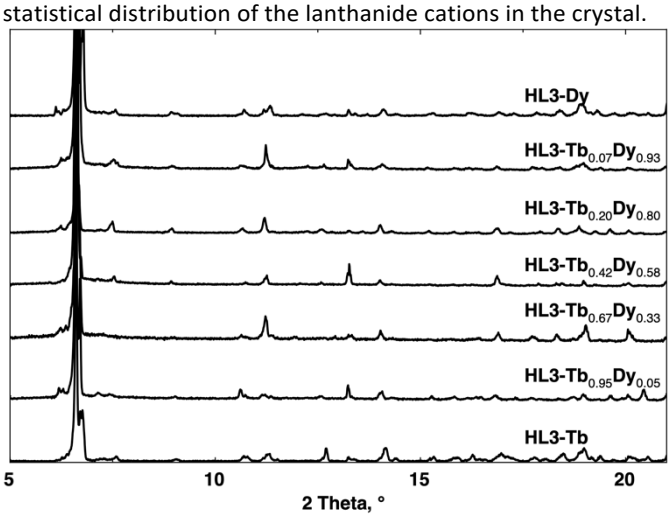

Figure 3. Comparison of the simulated for **HL3-Tb** (bottom) and **HL3-Dy** (top) and recorded PXRD patterns for $\mathbf{HL3\text{-}Tb_{1-x}Dy_x}$ solid solutions. Discrepancies in intensity between the observed and simulated patterns are due to preferential orientations of the microcrystalline powders.

The composition of the **HL3-Tb$_{1-x}$Dy$_x$** solid solutions has been checked using energy-dispersive X-ray spectroscopy (EDS), as shown in ESI.

Table 3: Comparison of the observed and experimental Tb/Dy ratios in **HL3-Tb$_{1-x}$Dy$_x$** Coordination Polymers.

	Tb/Dy experimental ratio	Tb/Dy observed ratio (EDS)
HL3-Tb$_{0.95}$Dy$_{0.05}$	95:05	95:05
HL3-Tb$_{0.67}$Dy$_{0.33}$	60:40	67:33
HL3- Tb$_{0.42}$Dy$_{0.58}$	40:60	42:58
HL3- Tb$_{0.20}$Dy$_{0.80}$	20:80	20:80
HL3- Tb$_{0.07}$Dy$_{0.93}$	10:90	07:93

The experimentally determined Tb/Dy ratios measured are in good agreement with the relative quantities of the lanthanide salts used for the synthesis. The slight differences are probably due to weighing uncertainty and overestimation of the Tb^{3+} content by the EDS measurements.

The properties of this series of compounds, luminescent and magnetic for **HL3-Dy**, are presented below.

Photoluminescence properties

For all investigated compounds, the measurements have been carried out in the solid state on polycrystalline powders.

The intensity of bands of the excitation spectra at RT for **HL3-Tb** and **HL3-Dy** in the 350-500 nm region with emission at λ_{em} = 534 nm and 576 nm respectively (see Figure S1, Supplementary Information) are attributed to the typical f-f transitions of Tb^{3+} and Dy^{3+} cations, that present lower intensities compared to the band attributed to $\pi \rightarrow \pi^*$ transitions of **H_4L3** (300-350 nm). These observations clearly indicate the occurrence of an energy transfer from the excited level of ligand **$HL3^{3-}$** to the emitting state of Tb^{3+} (or Dy^{3+}) cations, as seen in antenna effect.[77] The efficiency of calixarene carboxylate derivatives acting as antenna has already been reported for Tb^{3+} complexes.[53]

The room-temperature emission spectra of **HL3-Tb** and **HL3-Dy** coordination networks, when excited at λ_{ex} = 350 nm, are depicted in Figure 4. For **HL3-Tb**, the emission is composed of the characteristic five $^5D_4 \rightarrow {}^7F_6$, $^5D_4 \rightarrow {}^7F_5$ (strongest), $^5D_4 \rightarrow {}^7F_4$, $^5D_4 \rightarrow {}^7F_3$ and $^5D_4 \rightarrow {}^7F_2$ (weakest) electronic transitions, whereas for **HL3-Dy,** the $^4F_{9/2} \rightarrow {}^6H_{15/2}$, $^4F_{9/2} \rightarrow {}^6H_{13/2}$ (strongest) and $^4F_{9/2} \rightarrow {}^6H_{11/2}$ (weakest) electronic transitions are observed, as shown in Figures 4 a and b. These are typical f-f transitions, with emission in the green region for Tb^{3+} and in yellow white region for Dy^{3+}. The corresponding emission spectra at 77K are presented in Figures S2 a and b, Supplementary Information.

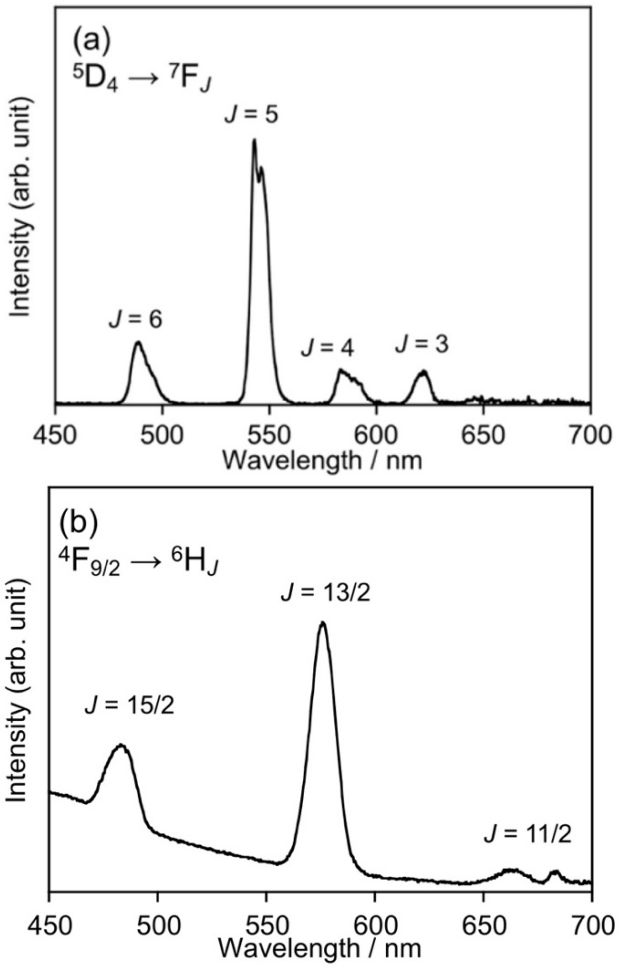

Figure 4. Emission spectra (λ_{ex} = 350 nm) of **HL3-Tb** (a) and **HL3-Dy** (b) at RT.

The photophysical behaviour of the mixed **HL3-Tb$_{1-x}$Dy$_x$** solid solutions was analysed at RT and at 77K. The luminescence spectra of the **HL3-Tb$_{1-x}$Dy$_x$** solid solution observed at RT and 77 K are shown in Figures 5 and S3.

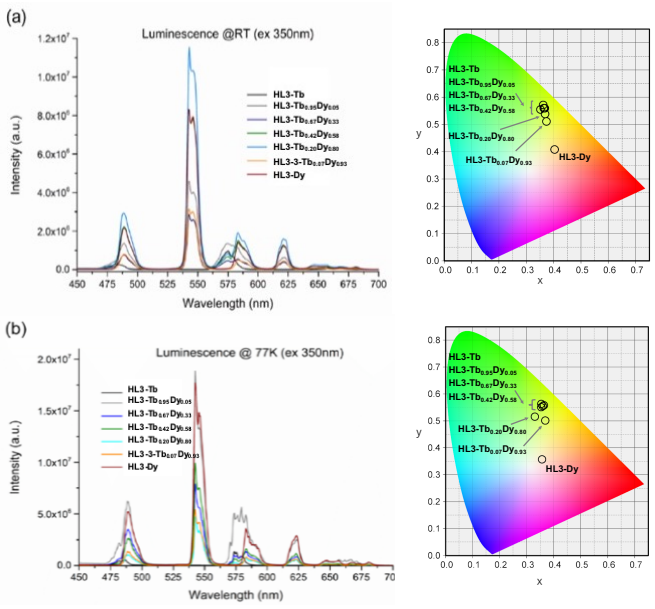

Figure 5. Emission spectra (λ_{ex} = 350 nm) of **HL3-Dy** (black) and **HL3-Tb** (brown), and solid solutions of **HL3-Tb$_{0.07}$Dy$_{0.93}$** (grey), **HL3-Tb$_{0.20}$Dy$_{0.80}$** (blue), **HL3-Tb$_{0.42}$Dy$_{0.58}$** (green), **HL3-Tb$_{0.67}$Dy$_{0.33}$** (light blue) and **HL3-Tb$_{0.95}$Dy$_{0.05}$** (orange) at room temperature (a) and at 77 K (b) and corresponding emission colours presented on the CIE 1931 chromaticity diagrams.

At RT, the **HL3-Tb$_{1-x}$Dy$_x$** solid solutions exhibits the typical luminescence bands assigned to f-f transitions of Tb^{3+} at 545 nm and of Dy^{3+} at 574 nm. The band intensities at 545 nm are decreasing when x is decreasing, and at 574 nm they are increasing when x is decreasing as shown in Figures 5 a and b. The luminescence of Dy^{3+} in these **HL3-Tb$_{1-x}$Dy$_x$** solid solutions cannot be obtained, due to extremely weak intensities, even at 77 K. The introduction of Dy^{3+} in **HL3-Tb$_{1-x}$Dy$_x$** solid solutions, allows a slight tuning of the emission colour in the **HL3-Tb$_{1-x}$Dy$_x$** solid solutions ranging from pale green to pale yellow, as shown in figures 5 a and b.

The absolute quantum yields of Tb^{3+} in a series of **HL3-Tb$_{1-x}$Dy$_x$** solid solutions were observed (see Figures S3 a and b, Supplementary Information), and the values at 77 K were found to be equal to 58.9% (27.9% at RT) for **HL3-Tb**, 32.6% for **HL3-Tb$_{0.95}$Dy$_{0.05}$**, 15.1% for **HL3-Tb$_{0.6}$Dy$_{0.4}$**. However, the existence of Dy^{3+} ion in the solid solution plays a role in decreasing the luminescence quantum yields of the **HL3-Tb$_{1-x}$Dy$_x$** solid solutions.

Luminescence decay profile and fitted results are summarized in Tables S2, S3 and Figures S3-S5 in ESI. As described above, the luminescence quantum yields of Dy^{3+} in the neat and solid solutions with Tb^{3+} are quite low and it was not possible to obtain the decay profiles at both RT and 77 K for **HL3-Dy**. The lifetimes of **HL3-Tb** at RT and 77 K were estimated as single component, with τ value of 0.866 and 0.916 ms, respectively. After addition of Dy^{3+} in **HL3-Tb$_{1-x}$Dy$_x$** solid solutions, the τ values are decreasing and the number of luminescence components of Tb^{3+} reach second or third (very fast) decay functions (see Tables S2 and S3 in ESI). The luminescence decay curve of **HL3-Tb$_{0.2}$Dy$_{0.8}$** can be divided into two, components, 0.378 and 0.932 ms (λ = 543 nm), at RT. The latter value corresponds to the one observed for **HL3-Tb**. The observation of second and third emission lifetimes is related to the increasing number of Dy^{3+} centers surrounding the Tb^{3+} centers.

The τ_{obs} values (Tables S2 and S3 in ESI) are in accordance with those reported for other calixarene based coordination compounds in the solid state.[53,78]

Magnetic measurements

As **HL3-Dy** contains magnetically anisotropic Dy^{3+} cations leading to a potential Single-Molecule Magnet character, its magnetic properties were investigated. The magnetic behaviour of **HL3-Tb**, because the lack of significant anisotropy for Tb, is not presented here. As shown in Figure 6, at 300 K, the $\chi_M T$ product reaches 14.1 $cm^3mol^{-1}K$, which is the exact value expected for the free-ion approximation. A typical decrease of the $\chi_M T$ product is observed upon cooling, which is related to the thermal depopulation within the m_J levels of the ground $^6H_{15/2}$ multiplet of Dy^{3+}. Beside slow decrease of the signal, the $\chi_M T$ versus T plot does not display abrupt changes which suggests the lack of magnetic interactions down to 1.8 K, as a result of efficient magnetic isolation of lanthanide centres in the crystal lattice. Magnetization measured at T = 1.8 K increases fast with increasing magnetic field to 10 kOe and much slower at higher fields reaching 5.4 μ_B at 60 kOe without saturation as expected for anisotropic Dy^{3+} (insert in Figure 6).[79]

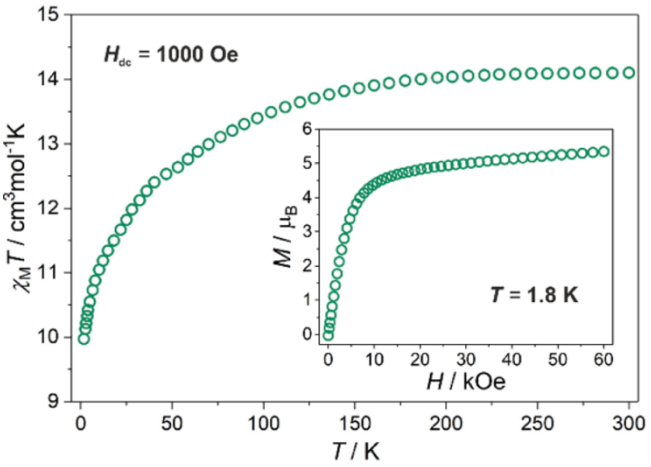

Figure 6. For **HL3-Dy**, temperature dependence of the χMT product at Hdc = 1000 Oe, and field dependence of molar magnetization at T = 1.8 K (inset).

To investigate the slow magnetic relaxation effects in 3-Dy, alternate-current (*ac*) magnetic characteristics were gathered at H_{dc}=0 (Figure 7a). The maxima at the frequency dependence of out-of-phase magnetic susceptibility, χ_M", appears on the edge of the measurement range, even at 1.8 K, quickly moving towards higher frequencies while the temperature increases. It indicates the presence of a slow magnetic relaxation, a characteristic effect of Single-Molecule Magnets (SMM) behaviour. To slow down the relaxation by reduction of presumably disturbing quantum tunnelling of magnetization (QTM) process, an external *dc* magnetic field was applied (see Figure S7, Supplementary Information). Field-variable *ac* magnetic characteristics were analysed using the generalized Debye model for a single relaxation.[80] The extracted relaxation times were plotted against magnetic field, and the resulting dependence was analysed taking into account QTM effect (Quantum Tunnelling of the Magnetisation) dominant at low fields and a field-induced direct process, responsible for the acceleration of relaxation process at highest fields (see Supplementary Information, Figure S7).[81] An equilibrium between these processes appears for H=1000 Oe, that was selected as the optimal one to investigate magnetic relaxation in 3-Dy. The *ac* magnetic characteristics were gathered in the 1.8-5 K temperature range (Figures 7b and see Supplementary Information, Figure S8). They were analysed using the generalized Debye model for a single relaxation, and the resulting relaxation times were presented in the function of temperature (Figure 7c).

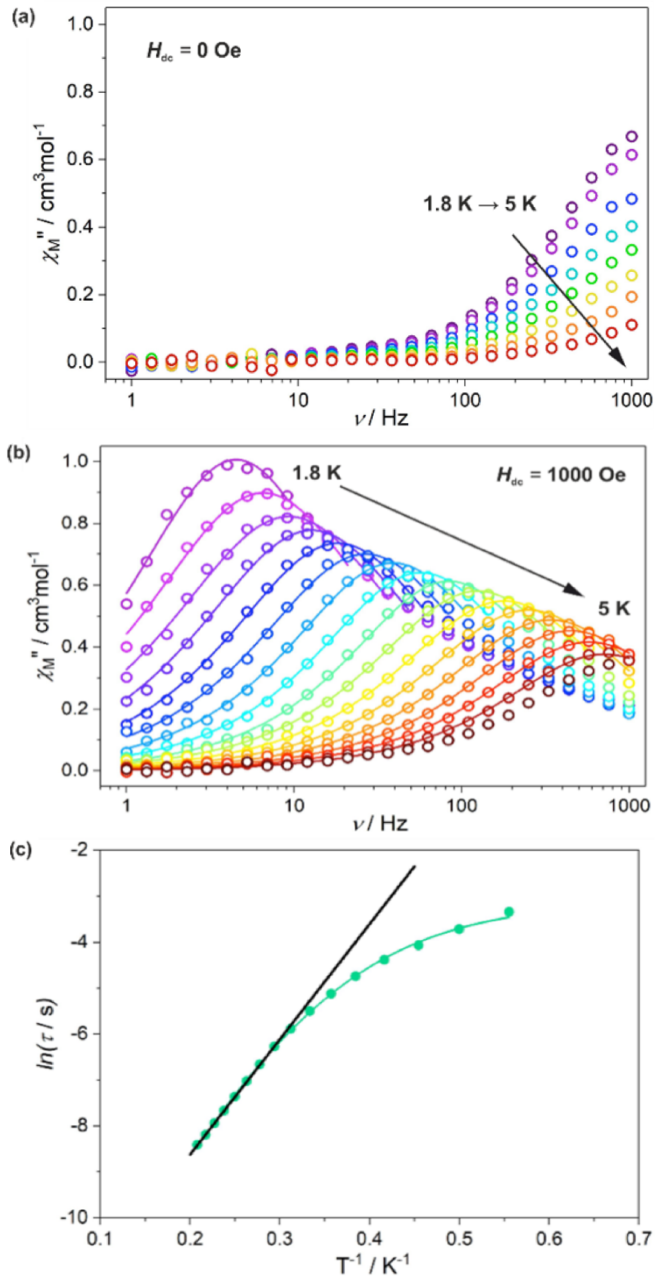

Figure 7. For **HL3-Dy**: zero *dc* field χ_M"(ν) curves in the range of 1.8–5 K (*a*), *dc* field χ_M"(ν) curves in the range 1.8-5 K under *dc* field of 1 kOe (b), and temperature dependence at 1 kOe of the relaxation time, τ (*c*), fitted using the Arrhenius law in the limited 3.4–5 K range (extrapolated black line) and within the full 1.8-5 K range using contributions from Orbach, Raman, direct and QTM relaxation processes. (green line; see text for details)

For the higher temperature range of 3.4-4.8 K, the temperature dependence of relaxation times is close linear, thus, it could be analysed by a simple Arrhenius law - the equation (1):

$$\ln(\tau) = \frac{U_{eff}}{k_B T} + \ln(\tau_0) \quad (1)$$

where U_{eff} represents an effective thermal energy barrier while τ_0 is the relaxation attempt time for spin reversal at infinite temperature. The obtained parameters of U_{eff}/k_B = 25.08(9) K, τ_0=1.2(2)·10^{-6} s are within the limits characteristic of Single-Molecule Magnets with moderate magnetic anisotropy.[79] More precisely, the full temperature dependence of relaxation times was fitted using contributions from Orbach and Raman relaxation processes, together with direct and QTM processes taken from the previous analysis of field-dependent relaxation. Therefore, the equation (2) was used:

$$\tau^{-1} = \tau_0^{-1}\exp(-U_{eff}/k_B T) + B_{Raman}T^n + \frac{a(1+c^2H^2)}{(1+bH^2)} + ATH^4 \quad (2)$$

where the first term represents an Orbach process related to the Arrhenius law, the second introduce a two-phonon Raman relaxation pathway, the third QTM effect and the last one shows a direct process.[82,83] To avoid over-parameterization, two last terms, describing QTM effect and a direct process, were taken from the field-dependence and the related parameters were not optimized during the fitting procedure (Figure S8). The obtained values of U_{eff}/k_B = 31(3) K and τ_0=1.2(7)·10^{-6} s are in the good agreement with those extracted from the Arrhenius law. The Raman process had to be included with B_{Raman} = 0.27(1) s^{-1}K^{-n}, n = 6.0(3), thus, the last value locates in the 2-9 range expected for lanthanide-based SMMs.[81] As several examples of SMMs lacking the Orbach process were reported,[84], we tried to fit the temperature dependence of relaxation times excluding Orbach process but it was not possible to obtain a satisficing fit. From these results, we can clearly postulate that Dy^{3+} complexes in **HL3-Dy** exhibits Single-Molecule Magnet characteristic with moderated thermal energy barrier originating from the Orbach relaxation process and strong QTM effect, partially reduced by using external *dc* magnetic field.

Conclusions

In this work, we demonstrated the possibility of growing a series of lanthanide based isostructural homometallic coordination polymers using thiacalix[4]arene bearing carboxylic moieties. Owing to their isostructural nature, a series of unprecedented heterometallic solid solutions, based on macrocyclic thiacalix[4]arene derivatives, has been generated. The two isostructural Tb^{3+} and Dy^{3+} based coordination polymers (**HL3-Tb** and **HL3-Dy**, formula [Ln^{III} **HL3**DMF$_3$]•(DMF)) have been structurally characterized using X-ray diffraction on single crystals and their photophysical properties have been investigated. The formation of the 1D ladder-type coordination compounds results specific binding of Ln^{3+} cation by the partially deprotonated organic tecton behaving as a "T-Shape" connector. For the solid solutions combing Tb^{3+} and Dy^{3+} leading **HL3-Tb$_{1-x}$Dy$_x$**, the Ln^{3+} cations are randomly distributed within the crystal.

The photoluminescence properties of the coordination polymers have been investigated. Ligand $HL3^{3-}$ sensitizes the luminescence of Tb^{3+} or Dy^{3+} cations in **HL3-Tb** and **HL3-Dy** at RT: they exhibit the characteristics f-f transition due to the presence of Ln^{3+} cations. The introduction of Dy^{3+} in **HL3-Tb** allows the tuning of the emission colour for solid solutions, between pale yellow and pale green.

In addition, magnetic measurements of **HL3-Dy** revealed a significant magnetic anisotropy of Dy^{3+} complexes attached to

thiacalix[4]arene moieties, leading to the SMM behaviour.

Therefore, this series of new Coordination Polymers can be considered as a novel source of bifunctional magneto-luminescent molecule-based materials.[85] We present a novel, elegant pathway for construction of luminescent molecular nanomagnets by incorporation of lanthanide ions in coordination chains based on functionalized thiacalix[4]arene ligands.

Experimental

X-Ray Crystallography

Data were collected at 173(2) K on a Bruker Apex-II-CCD diffractometer equipped with an Oxford Cryosystem liquid N_2 device, using graphite-monochromated Mo-Kα (λ = 0.71073 Å) radiation. For all structures, diffraction data were corrected for absorption. Structures were solved using SHELXS-97 and refined by full matrix least-squares on F^2 using SHELXL-97. Hydrogen atoms were introduced at calculated positions and refined using a riding model.[86] Structures can be obtained free of charge from the Cambridge Crystallographic Data Centre via www.ccdc.cam.ac.uk/datarequest/cif. CCDC: 1898825 (**HL3-Tb**) and 1898826 (**HL3-Dy**).

Powder diffraction studies (PXRD)

Diagrams were collected on a Bruker D8 diffractometer using monochromatic Cu-Kα radiation with a scanning range between 4 and 40° using a scan step size of 8° mn−1.

Elemental Analysis

Elemental analysis was performed by the Analysis Service of the Faculty of Chemistry of the University of Strasbourg.

EDS experiments

Elemental analyses using by EDS were performed on a Bruker-QUANTAX System, where EDS Detector was equipped with GEMINI FE-SEM ULTRA55 (Carl Zeiss). The samples were mixed with colloidal graphite in Isopropanol solution, dried and pressed into pellet. This EDS analysis worked on accelerating voltage of 15 kV.

Photophysical properties

Luminescence and excitation spectra were recorded on a Fluorolog 3-22 (Horiba Jobin Yvon).

Absolute luminescence quantum yields and luminescence lifetimes were determined using an absolute luminescence quantum yield spectrometer C9920-02 (Hamamatsu Photonics K. K.) and a Quantaurus-Tau C11367-12 (Hamamatsu Photonics K. K.), respectively, with pulsed excitation light sources.

Magnetic properties

Magnetic properties were investigated by using a Quantum Design MPMS-3 Evercool magnetometer on the powder sample of **HL3-Dy** dispersed in paraffin oil to avoid the rotation of the crystals under an magnetic field. Magnetic data were corrected for the diamagnetic contributions from the sample, oil and the sample holder.

Synthesis

All reagents were purchased from commercial sources and used without further purification. **H_4L3** was prepared using a modified previously reported procedure.[63,74]

Crystallization conditions

3-Tb: A solution containing **H_4L3** (5 mg, 0.005 mmol) dissolved in DMF (1 ml) was mixed with a 0.01 M solution of $Tb(NO_3)_3$•$6H_2O$ in DMF (1 ml, 0.01 mmol). Then 2 drops of 1M HCl were added to the mixture. In a vial closed with a cap, the solution was heated at 80 °C during 3 days, and after cooling to RT, colourless single crystals were obtained (5,3 mg, 73%), filtrated and washed with DMF (2 ml) and diethyl ether (2 ml). Formula: $C_{60}H_{81}TbN_4O_{16}S_4$, Anal. Calcd.: C, 51.42%; H, 5.83%; N, 4.00%; Found: C, 51.45%; H, 5.87%; N, 4.06%.

HL3-$Tb_{0.95}Dy_{0.05}$: The same procedure was applied starting from a 0.01 M solution of $Tb(NO_3)_3$•$6H_2O$ in DMF (0.95 ml, 0.0095 mmol) and a 0.01 M solution of $Dy(NO_3)_3$•$5H_2O$ (0.05 ml, 0.005 mmol). Yield, 4,6 mg (64%). Formula: $C_{60}H_{81}Tb_{0.05}Dy_{0.95}N_4O_{16}S_4$, Anal. Calcd.: C, 51.30%; H, 5.81%; N, 3.99%; Found: C, 51.38%; H, 5.85%; N, 4.05%.

HL3-$Tb_{0.67}Dy_{0.33}$: The same procedure was applied starting from a 0.01 M solution of $Tb(NO_3)_3$•$6H_2O$ in DMF (0.75 ml, 0.0075 mmol) and a 0.01 M solution of $Dy(NO_3)_3$•$5H_2O$ (0.25 ml, 0.0025 mmol). Yield, 4.5 mg (62%). Formula: $C_{60}H_{81}Tb_{0.67}Dy_{0.33}N_4O_{16}S_4$, Anal. Calcd.: C, 51.38%; H, 5.82%; N, 4.00%; Found: C, 51.42%; H, 5.96%; N, 4.08%.

HL3-$Tb_{0.42}Dy_{0.58}$: The same procedure was applied starting from a 0.01 M solution of $Tb(NO_3)_3$•$6H_2O$ in DMF (0.5 ml, 0.005 mmol) and a 0.01 M solution of $Dy(NO_3)_3$•$5H_2O$ (0.5 ml, 0.005 mmol). Yield, 5.2 mg (65%). Formula: $C_{60}H_{81}Tb_{0.42}Dy_{0.58}N_4O_{16}S_4$, Anal. Calcd.: C, 51.35%; H, 5.82%; N, 3.99%; Found: C, 51.52%; H, 5.85%; N, 3.98%.

HL3-$Tb_{0.2}Dy_{0.8}$: The same procedure was applied starting from a 0.01 M solution of $Tb(NO_3)_3$•$6H_2O$ in DMF (0.25 ml, 0.0025 mmol) and a 0.01 M solution of $Dy(NO_3)_3$•$5H_2O$ (0.75 ml, 0.0075 mmol). Yield, 5.8 mg (75%). Formula: $C_{60}H_{81}Tb_{0.2}Dy_{0.8}N_4O_{16}S_4$, Anal. Calcd.: C, 51.32%; H, 5.81%; N, 3.99%; Found: C, 51.39%; H, 5.83%; N, 4.02%

HL3-$Tb_{0.07}Dy_{0.93}$: The same procedure was applied starting from a 0.01 M solution of $Tb(NO_3)_3$•$6H_2O$ in DMF (0.1 ml, 0.001 mmol) and a 0.01 M solution of $Dy(NO_3)_3$•$5H_2O$ (0.9 ml, 0.009 mmol). Yield, 5.3 mg (73%). Formula: $C_{60}H_{81}Tb_{0.07}Dy_{0.93}N_4O_{16}S_4$, Anal. Calcd.: C, 51.30%; H, 5.81%; N, 3.99%; Found: C, 51.45%; H, 5.79%; N, 4.08%

HL3-Dy: The same procedure was applied starting from a 0.01 M solution of $Dy(NO_3)_3$•$5H_2O$ in DMF (1 ml, 0.01 mmol). Yield, 4.8 mg (68%). Formula: $C_{60}H_{81}O_{16}N_4S_4Dy$, Anal. Calcd.: C, 51.29%; H, 5.81%; N, 3.99%; Found: C, 51.35 %; H, 5.86 %; N, 4.02 %.

Conflicts of interest

There are no conflicts to declare.

Acknowledgements

We thank the Russian Science Foundation (grant N° 17-73-20117) for financial support for the synthesis and crystal preparation. Financial supports from the University of

Strasbourg, the International Centre for Frontier Research in Chemistry (icFRC), Laboratory of excellence LabEx CSC, Strasbourg, the Institut Universitaire de France, the CNRS, and MEXT Grants-in-Aid for Scientific Research on Innovative Areas of "Soft Crystals (Area Number: 2903, No. 17H06374) are acknowledged. Center for Instrumental Analysis, College of Science and Engineering, Aoyama Gakuin University also supports to analyse EDS.

Notes and references

1 B. F. Abrahams, B. F. Hoskins, R. Robson, A new type of infinite 3D polymeric network containing 4-connected, peripherally-linked metalloporphyrin building blocks, *J. Am. Chem. Soc*. 1991, **113**, 3606-3607.

2 S. R. Batten, R. Robson, Interpenetrating Nets: Ordered, Periodic Entanglement, *Angew. Chem. Int. Ed*. 1998, **37**, 1460-1494.

3 *Chem. Rev*., 2012, **112**, Metal-Organic Frameworks special issue.

4 M. W. Hosseini, Reflexion on molecular tectonics, *CrystEngComm*, 2004, **6**, 318-322.

5 M. W. Hosseini, Molecular Tectonics: From Simple Tectons to Complex Molecular Networks, *Acc. Chem. Res*., 2005, **38**, 313-323.

6 G. Férey, C. Serre, T. Devic, G. Maurin, H. Jobic, P.L. Llewellyn, G. De Weireld, A. Vimont, M. Daturi, J.-S. Chang, Why hybrid porous solids capture greenhouse gases?, *Chem. Soc. Rev*. 2011, **40**, 550-562.

7 H.-C. Zhou, J.R. Long, O.M. Yaghi, Introduction to Metal–Organic Frameworks, *Chem. Rev*. 2012, **112**, 673-674.

8 L.Q. Ma, C. Abney, W.B. Lin, Enantioselective catalysis with homochiral metal–organic frameworks, *Chem. Soc. Rev*. 2009, **38**, 1248-1256.

9 M. Yoon, R. Srirambalaji, K. Kim, Homochiral Metal–Organic Frameworks for Asymmetric Heterogeneous Catalysis, *Chem. Rev*. 2012, **112**, 1196-1231.

10 P. Dechambenoit, J. R. Long, Microporous magnets, *Chem. Soc. Rev*. 2011, **40**, 3249-3265 .

11 G. M Espallargas, E. Coronado Magnetic functionalities in MOFs: from the framework to the pore, *Chem. Soc. Rev*., 2018, **47**, 533-557.

12 M.D. Allendorf, C.A. Bauer, R.K. Bhakta, R.J.T. Houk, Luminescent metal–organic frameworks, *Chem. Soc. Rev*. 2009, **38**, 1330-1352.

13 B. Chen, S. Xiang, G. Qian, Metal−Organic Frameworks with Functional Pores for Recognition of Small Molecules, *Acc. Chem. Res.* 2010, **43**, 1115-1124.

14 Y. Cui, Y. Yue, G. Qian, B. Chen, Luminescent Functional Metal–Organic Frameworks, *Chem. R*ev. 2012, **112**, 1126-1162.

15 *Advances in Inorganic chemistry, Supramolecular Chemistry*, eds R. van Eldik, R. Puchta, academic press, 2018.

16 J. Rocha, L. D. Carlos, F. A. A. Paz, D. Ananias, Luminescent multifunctional lanthanides-based metal–organic frameworks, *Chem. Soc. Rev*. **2011**, *40*, 926-940.

17 Y. Cui, B. Chen, G. Qian Lanthanide metal-organic frameworks for luminescent sensing and light-emitting applications, *Coord. Chem. Rev*. 2014, **273-274**, 76-86.

18 Y. Cui, B. Li, H. He, W. Zhou, B. Chen, G. Qian, Metal–Organic Frameworks as Platforms for Functional Materials**,** *Acc. Chem. Res*. 2016, **49**, 483-493.

19 S. Roy, A. Chakraborty, T. K. Maji Qian, Lanthanide–organic frameworks for gas storage and as magneto-luminescent materials, *Coord. Chem. Rev*. 2014, **273-274**, 139-.

20 Y. Hasegawa, T. Nakanishi, Luminescent lanthanide coordination polymers for photonic applications, *RSC Adv*. 2015, **5**, 338-353.

21 J. Wu, H. Zhang, S. Du, Tunable luminescence and white light emission of mixed lanthanide–organic frameworks based on polycarboxylate ligands, *J. Mater. Chem. C*, 2016, **1**, 3364-3374.

22 S. Tobita, M. Arakawa, I. Tanaka, The paramagnetic metal effect on the ligand localized S1 .apprx. .fwdarw. T1 intersystem crossing in the rare-earth-metal complexes with methyl salicylate, *J. Phys. Chem*, 1985, **89**, 5649-5654.

23 J. C. G. Bünzli, Review: Lanthanide coordination chemistry: from old concepts to coordination polymers, *J. Coord. Chem*. 2014, **67**, 3706-3733.

24 Q. Zha , X. Rui , T. Wei, Y. Xie, Recent advances in the design strategies for porphyrin-based coordination polymers, *CrystEngComm* 2014, ***16***, 7371-7384.

25 J. J. Baldovi, E. Coronado, A. Gaita-Arino, C. Gamer, M. Gimenez-Marques, G. Minguez Espallargas, A SIM-MOF: Three-Dimensional Organisation of Single-Ion Magnets with Anion-Exchange Capabilities, *Chem. Eur. J*. 2014, **20**, 10695-10702.

26 X. Zhang, V. Vieru, X. Feng, J.-L. Liu, Z. Zhang, B. Na, W. Shi, B.-W. Wang, A. K. Powell, L. F. Chibotaru, S. Gao, P. Cheng, J. R. Long, Influence of Guest Exchange on the Magnetization Dynamics of Dilanthanide Single-Molecule-Magnet Nodes within a Metal-Organic Framework, *Angew. Chem. Int. Ed.* 2015, **54**, 9861-9865.

27 D.-D. Yin, Q. Chen, Y.-S. Meng, H.-L. Sun, Y.-Q. Zhang, S. Gao, Slow magnetic relaxation in a novel carboxylate/oxalate/hydroxyl bridged dysprosium layer, *Chem. Sci*. 2015, **6**, 3095-3101.

28 S. Mohapatra, B. Rajeswaran, A. Chakraborty, A. Sundaresan, T. K. Maji, Bimodal Magneto-Luminescent Dysprosium (DyIII)-Potassium (KI)-Oxalate Framework: Magnetic Switchability with High Anisotropic Barrier and Solvent Sensing, *Chem. Mater*. 2013, **25**, 1673-1679.

29 R. Jankowski, J. J. Zakrzewski, O. Surma, S. Ohkoshi, S. Chorazy, B. Sieklucka, Near-infrared emissive Er(iii) and Yb(iii) molecular nanomagnets in metal–organic chains functionalized by octacyanidometallates(iv), *Inorg. Chem. Front*. 2019, **6**, 2423-2434.

30 Y. Xin, J. Wang, M. Zychowicz, J. J. Zakrzewski, K. Nakabayashi, B. Sieklucka, S. Chorazy, S. Ohkoshi, Dehydration–Hydration Switching of Single-Molecule Magnet Behavior and Visible Photoluminescence in a Cyanido-Bridged DyIIICoIII Framework*J. Am. Chem. Soc.* 2019, **141**, 18211-18220.

31 C. D. Gutsche in *Calixarenes Revised: Monographs in Supramolecular Chemistry Vol. 6*, The Royal Society of Chemistry, Cambridge, 1998.

32 Z. Asfari, V. Böhmer, J. Harrowfield and J. Vicens in *Calixarenes 2001*, (Eds. Z. Asfari, V. Böhmer, J. Harrowfield and J. Vicens) Kluwer Academic, Dordrecht, 2001.

33 M. W. Hosseini, ACS Series, Eds G. J. Lumetta, R. D. Rogers, A. S. Gopalan, 2000, ***557***, 296.

34 H. Kumagai, M. Hasegawa, S. Miyanari, Y. Sugawa, Y. Sato, T. Hori, S. Ueda, H. Kamiyama, S. Miyano, Facile synthesis of p-tert-butylthiacalix[4]arene by the reaction of p-tert-butylphenol with elemental sulfur in the presence of a base, *Tetrahedron Lett*. 1997, **38**, 3971-3972.

35 P. Rao, M. W. Hosseini, A. De Cian, J. Fischer, Synthesis and structural analysis of mercaptothiacalix[4]arene, *Chem. Commun*. 1999, 2169-2170.

36 H. Akdas, E. Graf, M. W. Hosseini, A. de Cian, A. Bilyk, B. W. Skelton, G. A. Koutsantonis, I. Murray, J. M. Harrowfield, A. H. White, Koilands from thiophiles: mercury(ii) clusters from thiacalixarenes, *Chem. Commun*. 2002, 1042-1043.

37 A. Ovsyannikov, S. Solovieva, I. Antipin, S. Ferlay, Coordination Polymers based on calixarene derivatives: Structures and properties, *Coord. Chem. Rev*., 2017, **352**, 151-186.

38 F.M. Ramirez, L. Charbonnière, G. Muller, J-C. G. Bünzli, Tuning the Stoichiometry of Lanthanide Complexes with Calixarenes: Bimetallic Complexes with a Calix[6]arene Bearing Ether-Amide Pendant Arms, *Eur. J. Inorg. Chem*. 2004, 2348-2355.

39 K. Z. Su, F. L. Jiang, J. J. Qian, J. D. Pang, F. L. Hu, S. M. Bawaked, M. Mokhtar, S. A. Al-Thabaiti, M. Hong, Synthesis and characterization of decanuclear Ln(III) cluster of mixed calix[8]arene-phosphonate ligands (Ln = Pr, Nd), *Inorg. Chem. Commun*. 2015, **54**, 34-37.

40 T. Kajiwara, N. Iki, M. Yamashita, Transition metal and lanthanide cluster complexes constructed with thiacalix[n]arene and its derivatives, *Coord. Chem. Rev*. 2007, **251**, 1734-1746.

41 B. S. Creavena, D. F. Donlona, J. McGinley, Coordination chemistry of calix[4]arene derivatives with lower rim functionalisation and their applications, *Coord. Chem. Rev*. 2009, **253**, 893-962.

42 S. Sanz, R. D. McIntosh, C. M. Beavers, S. J. Teat, M. Evangelisti, E. K. Brechin, S. J. Dalgarno, Calix[4]arene-supported rare earth octahedra, *Chem. Commun*. 2012, **48**, 1449-1451.

43 J. P. Chinta, B. Ramanujam, C. P. Rao, Structural aspects of the metal ion complexes of the conjugates of calix[4]arene: Crystal structures and computational models, *Coord. Chem. Rev*., 2012, **256**, 2762-2794.

44 Y.F. Bi, Y.L. Li, W.P. Liao, H.J. Zhang, D.Q. Li, A Unique Mn2Gd2 Tetranuclear Compound of p-tert-Butylthiacalix[4]arene, *Inorg. Chem*. 2008, **47**, 9733-9734.

45 Y.F. Bi, X.T. Wang, B.W. Wang, W.P. Liao, X.F. Wang, H.J. Zhang, S. Gao, D.Q. Li, Two MnII2LnIII4 (Ln = Gd, Eu) hexanuclear compounds of p-tert-butylsulfinylcalix[4]arene, *Dalton Trans*. 2009, **12**, 2250-2254.

46 G. Karotsis, S. Kennedy, S. J. Teat, C. M. Beavers, D. A. Fowler, J. J. Morales, M. Evangelisti, S. J. Dalgarno, E. K. Brechin, [MnIII4LnIII4] Calix[4]arene Clusters as Enhanced Magnetic Coolers and Molecular Magnets, *J. Am. Chem. Soc.* 2010, **132**, 12983-12990.

47 S. Sanz, K. Ferreira, R. D. McIntosh, S. J. Dalgarno, E. K. Brechin, Calix[4]arene-supported FeIII2LnIII2 clusters, *Chem. Commun*. 2011, **47**, 9042-9044.

48 Y. Bi, S. Du, W. Liao, Thiacalixarene-based nanoscale polyhedral coordination cages, *Coord. Chem. Rev*. 2014, **276**, 61-72.

49 M. Coletta, R. McLellan, A. Waddington, S. Sanz, K. J. Gagnon, S. J. Teat, E. K. Brechin, S. J. Dalgarno, Core expansion of bis-calix[4]arene-supported clusters, *Chem. Commun*. 2016, **52**, 14246-14249.

50 M. Coletta, R. McLellan, S. Sanz, K. J. Gagnon, S. J. Teat, E. K. Brechin, S. J. Dalgarno, A New Family of 3d–4f Bis-Calix[4]arene-Supported Clusters, *Chem. Eur. J*., 2017, **23**, 14073-14079.

51 H. Han, X. Li, X. Zhu, G. Zhang, S. Wang, X. Hang, J. Tang, W. Liao, Single-Molecule-Magnet Behavior in a Calix[8]arene-Capped {Tb6IIICrIII} Cluster, *Eur. J. Inorg. Chem.* 2017, 2088-2093.

52 A. Jäschke, M. Kischel, A. Mansel, B. Kersting, Hydroxyquinoline–Calix[4]arene Conjugates as Ligands for Polynuclear Lanthanide Complexes: Preparation, Characterization, and Properties of a Dinuclear EuIII Complex, *Eur. J. Inorg. Chem.* 2017, 894-901.

53 R.S. Viana, C.A.F. Oliveira, J. Chojnacki, B. S. Barros, S. Alves-Jr, J. Kulesza, Structural and spectroscopic investigation of new luminescent hybrid materials based on calix[4]arene-tetracarboxylate and Ln3+ ions (Ln = Gd, Tb or Eu), *J. Solid St. Chem*., 2017, **251**, 26-32.

54 S. J. Dalgarno, M. J. Hardie, J. L. Atwood, C. L. Raston, Bilayers, Corrugated Bilayers, and Coordination Polymers of p-Sulfonatocalix[6]arene, *Inorg. Chem*. 2004, **43**, 6351-6356.

55 W. Liao, C. Liu, X. Wang, G. Zhu, X. Zhao, H. Zhang, 3D metal–organic frameworks incorporating water-soluble tetra-p-sulfonatocalix[4]arene, *CrystEngComm*. 2009, **11**, 2282-2284.

56 I. Ling, Y. Alias, C. L. Raston, Structural diversity of multi-component self-assembled systems incorporating p-sulfonatocalix[4]arene, *N. J. Chem*. 2010, **34**, 1802-1811.

57 I. Ling, C. L. Raston, Primary and secondary directing interactions of aquated lanthanide(III) ions with p-sulfonated calix[n]arene, *Coord. Chem. Rev*. 2018, **375**, 80-105.

58 K. Kim, S. Park, K.-M. Park, K.-M. Park, S.S. Lee, Thiacalix[4]arene-Based Three-Dimensional Coordination Polymers Incorporating Neutral Bridging Coligands, *Cryst. Growth Des*., 2011, **11**, 4059-4067.

59 Z. Zhang, A. Drapailo, Y. Matvieiev, L. Wojtas, M.J. Zaworotko, A calixarene based metal organic material, calixMOM, that binds potassium cations, *Chem. Commun*. 2013, 8353-8355.

60 H. Akdas, E. Graf, M.W. Hosseini, A. De Cian, J.McB. Harrowfield, Design, synthesis and structural investigation of a 2-D coordination network based on the self-assembly of the tetracarboxylate derivative of tetrathiacalix[4]arene. *Commun*. 2000, 2219-2220.

61 J.-Y. Kim, K. Kim, K.-M. Park, S.S. Lee, Isostructural Heteronuclear (K+/M2+: M = Ni, Co, and Zn) One-Dimensional Coordination Polymers of Thiacalix[4]arene Tetraacetate, *Bull. Korean Chem. Soc*. 2014, **35**, 289-292.

62 A.S. Ovsyannikov, S. Ferlay, S. E. Solovieva, I. S. Antipin, A. I. Konovalov, N. Kyritsakas, M. W. Hosseini, Molecular tectonics: high dimensional coordination networks based on methylenecarboxylate-appended tetramercaptothiacalix[4]arene in the 1,3-alternate conformation, C*rystEngComm* 2018, **20**, 1130-1140.

63 A.S. Ovsyannikov, M. Lang, S. Ferlay, S. E. Solovieva, I. S. Antipin, A. I. Konovalov, N. Kyritsakas, M. W. Hosseini, Molecular tectonics: tetracarboxythiacalix[4]arene derivatives as tectons for the formation of hydrogen-bonded networks, *CrystEngComm* 2016, **18**, 8622-8630.

64 K.A. White, D.A. Chengelis, K.A. Gogick, J. Stehman, N.L. Rosi, S. Petoud, Near-Infrared Luminescent Lanthanide MOF Barcodes, *J. Am. Chem. Soc*. 2009, **131**, 18069-18071.

65 S. Dang, J. H. Zhang, Z. M. Sun, Tunable emission based on lanthanide(iii) metal–organic frameworks: an alternative approach to white light, *J. Mater. Chem*. 2012, **22**, 8868-8873.

66 V. Haquin, M. Etienne, C. Daiguebonne, S. Freslon, G. Calvez, K. Bernot, L. Le Pollès, S. E. Ashbrook, M. R. Mitchell, J.-C. Bünzli, S. V. Eliseeva, O. Guillou, Color and Brightness Tuning in Heteronuclear Lanthanide Terephthalate Coordination Polymers *Eur. J. Inorg. Chem*. 2013, 3464-3476.

67 D.T. de Lill, N.S. Gunning, C.L. Cahill, Toward Templated Metal−Organic Frameworks: Synthesis, Structures, Thermal Properties, and Luminescence of Three Novel Lanthanide−Adipate Frameworks, *Inorg. Chem*. 2005, **44**, 258-266.

68 K. Liu, H. You, Y. Zheng, G. Jia, Y. Song, Y. Huang, M. Yang, J. Jia, N. Guo, H. Zhang, Facile and rapid fabrication of metal–organic framework

nanobelts and color-tunable photoluminescence properties, *J. Mater. Chem*. 2010, **20**, 3272-3279.

69 S. Mohapatra, S. Adhikari, H. Riju, T.K. Maji, Terbium(III), Europium(III), and Mixed Terbium(III)–Europium(III) Mucicate Frameworks: Hydrophilicity and Stoichiometry-Dependent Color Tunability, *Inorg. Chem*. 2012, **51**, 4891-4893.

70 Y. Cui, H. Xu, Y. Yue, Z. Guo, J. Yu, Z. Chen, J. Gao, Y. Yang, G. Qian, B. Chen, A Luminescent Mixed-Lanthanide Metal–Organic Framework Thermometer, *J. Am. Chem. Soc*. 2012, **134**, 3979-3982.

71 A. R. Ramya, D. Sharma, S. Natarajan, M. L. P. Reddy, Highly Luminescent and Thermally Stable Lanthanide Coordination Polymers Designed from 4-(Dipyridin-2-yl)aminobenzoate: Efficient Energy Transfer from Tb3+ to Eu3+ in a Mixed Lanthanide Coordination Compound, *Inorg. Chem*. 2012, **51**, 8818-8826.

72 S. Sato, A. Ishii, C. Yamada, J. Kim, H. S. Chul, A. Fujiwara, M. Takata, M. Hasegawa, Luminescence of fusion materials of polymeric chain-structured lanthanide complexes, *Polymer J*., 2015, **47**, 195-200.

73 K. Kumar, S. Chorazy, K. Nakabayashi, H. Sato, B. Sieklucka, S.-I. Ohkoshi, TbCo and Tb0.5Dy0.5Co layered cyanido-bridged frameworks for construction of colorimetric and ratiometric luminescent thermometers, *J. Mater. Chem. C*, 2018, **6**, 8372-8384

74 H. Akdas, G. Mislin, E. Graf, M. Hosseini, A. De Cian, J. Fisher, Synthesis and solid state structural analysis of conformers of tetrakis((ethoxycarbonyl)methoxy)tetrathiacalix[4]arene, *Tetrahedron Lett*. 1999, **40**, 2113-2116.

75 N. Iki, N. Morohashi, F. Narumi, T. Fujimoto, T. Suzuki, S. Miyano, Novel molecular receptors based on a thiacalix[4]arene platform. Preparations of the di- and tetracarboxylic acid derivatives and their binding properties towards transition metal ions, *Tetrahedron Lett*. 1999, **40**, 7337-7341.

76 The program is available free of charge at http://www.ee.ub.edu/.

77 G. F. de Sá, O. L. Malta, C. M. Donegá, A. M. Simas, R. L. Longo, P. A. Santa-Cruz, E. F. da Silva Jr, Spectroscopic properties and design of highly luminescent lanthanide coordination complexes, *Coord. Chem. Rev*., 2000, **196,** 165-195.

78 M. F. Hazenkamp, G. Blasse, N. Sabbatini, R. Ungaro, The solid state luminescence of the encapsulation complex of Eu3+ in p-t-butyl-calix[4] arene tetra-amide, *Inorg. Chim. Acta*, 1990, **172**, 93-95.

79 D. Woodruff, R. E. P. Winpenny, R. A. Layfield, Lanthanide Single-Molecule Magnets, *Chem. Rev.* 2013, **113**, 5110-5148.

80 Y.-N. Guo, G.-F. Xu, Y. Guo, J. Tang, Relaxation dynamics of dysprosium(iii) single molecule magnets, *Dalton Trans.* 2011, **40**, 9953-9963.

81 A. Amjad, A. Figuerola, L. Sorace, Tm(iii) complexes undergoing slow relaxation of magnetization: exchange coupling and aging effects, *Dalton Trans.* 2017, **46**, 3848-3856.

82 K. S. Pedersen, J. Dreiser, H. Weihe, R. Sibile, H. V. Johannesen, M. A. Sorensen, B. E. Nielsen, M. Sigrist, H. Mutka, S. Rols, J. Bendix, S. Piligkos, Design of Single-Molecule Magnets: Insufficiency of the Anisotropy Barrier as the Sole Criterion, *Inorg. Chem.* 2015, **54**, 7600-7606.

83 S. Chorazy, J. J. Zakrzewski, M. Reczyński, K. Nakabayashi, S. Ohkoshi, B. Sieklucka, Humidity driven molecular switch based on photoluminescent DyIIICoIII single-molecule magnets, *J. Mater. Chem. C* 2019, **7**, 4164-4172.

84 J. J. Zakrzewski, S. Chorazy, K. Nakabayashi, S. Ohkoshi, B. Sieklucka, Photoluminescent Lanthanide(III) Single-Molecule Magnets in Three-Dimensional Polycyanidocuprate(I)-Based Frameworks, *Chem. Eur. J.* 2019, **25**, 11820-11825.

85 J-H. Jia, Q-W. Li, Y-C. Chen, J-L. Liu, M-L. Tong, Luminescent single-molecule magnets based on lanthanides: Design strategies, recent advances and magneto-luminescent studies, *Coord. Chem. Rev*., 2019, **378**, 365-381.

86 G. M. Sheldrick, A short history of SHELX *Acta Crystallogr.* **2008**, *A64*, 112-122.

ARTICLE

Table 1: Crystallographic Parameters for **HL3-Dy and HL3-Tb** recorded at 173 K.

Formula	$C_{48}H_{53}O_{12}S_4Dy(C_3H_7NO)_3$, C_3H_7NO $C_{60}H_{81}DyN_4O_{16}S_4$ **HL3-Dy**	$C_{48}H_{53}O_{12}S_4Tb(C_3H_7NO)_3$, C_3H_7NO $C_{60}H_{81}TbN_4O_{16}S_4$ **HL3-Tb**
Molecular weight	1405.02	1401.44
Crystal system	Triclinic	Triclinic
Space group	*P*-1	*P*-1
a(Å)	15.0091(17)	15.0160(17)
b(Å)	15.9798(18)	15.9630(14)
c(Å)	16.7401(18) Å	16.7660(16)
α(deg)	62.217(5)	62.226(3)
β(deg)	67.626(5)	67.513(3)
γ(deg)	79.181(6)	79.132(4)°
V(Å^3)	3284.5(7)	3285.2(6)
Z	2	2
Colour	Colourless	Colourless
Crystal dim (mm^3)	0.090 x 0.100 x 0.100	0.090 x 0.100 x 0.100
Dcalc (gcm^{-3})	1.421	1.417
F(000)	1454	1452
μ (mm^{-1})	1.332	1.270
Wavelength (Å)	0.71073	0.71073
Number of data meas.	83469	36284
Number of data with I> 2σ(I)	17032 [R(int) = 0.0752]	17822 [R(int) = 0.0558]
R	R1 = 0.0557, wR2 = 0.1391	R1 = 0.0494, wR2 = 0.1073
Rw	R1 = 0.0756, wR2 = 0.1559	R1 = 0.0708, wR2 = 0.1186
GOF	1.057	1.011
Largest peak in final difference (eÅ^{-3})	1.740 and -1.406	1.411 and -1.140

GRAPHICAL ABSTRACT